Spectroscopy on Thick HgI_2 Detectors: A Comparison Between Planar and Pixelated Electrodes

James E. Baciak, *Student Member, IEEE,* and Zhong He, *Senior Member, IEEE*

Abstract—Thick mercuric iodide (HgI_2) detectors are investigated as potential room temperature gamma-ray spectrometers. By using pixelated anodes the induced charge on the electrode is dependent mainly on electron movement and is almost independent of the depth of interaction. Moreover, by reading out the planar cathode signal simultaneously, the depth of interaction can be determined and any effects of electron charge loss can be corrected. By combining these two methods (pixelated anodes and depth sensing), the resolution from 1 cm thick HgI_2 devices can be improved to 1.4% FWHM when using a Cs-137 point source. These results were obtained using a modest electric field (2500 V/cm) and relatively short shaping times (4–16 μs) for HgI_2. A comparison between conventional planar readout and single polarity charge sensing techniques with wide band-gap semiconductors is discussed.

Index Terms—Gamma-ray spectroscopy, mercuric iodide, room temperature.

I. INTRODUCTION

MERCURIC IODIDE (HgI_2) crystals have been studied as a potential gamma-ray spectrometer that can operate at room temperature [1], [2] for approximately 30 years. Like many compound semiconductor materials, HgI_2 suffers from poor charge transportation characteristics. HgI_2 has a wide bandgap (2.1 eV), high atomic numbers (53 for iodine, 80 for mercury), and a high density (6.4 g/cm^3). However, the crystals suffer from low electron and hole mobility, significant hole trapping, and material nonuniformity. Thus, HgI_2 detectors using conventional planar electrodes have been limited to thicknesses much less than 1 cm with high applied voltages when operating as a spectrometer due to incomplete charge collection. To improve the spectroscopic performance of thick HgI_2 detectors, one must reduce the depth dependence of the generated pulse.

One such method, single-polarity charge sensing, was implemented in order to overcome the severe hole trapping present in wide bandgap semiconductor detectors, including HgI_2. The introduction of pixelated anodes to CdZnTe [3], [4] showed that the resolution of wide bandgap semiconductor detectors can be dramatically improved compared to standard planar electrode configuration. By measuring the signal from the planar cathode and anode pixels concurrently, interaction depth information [5]
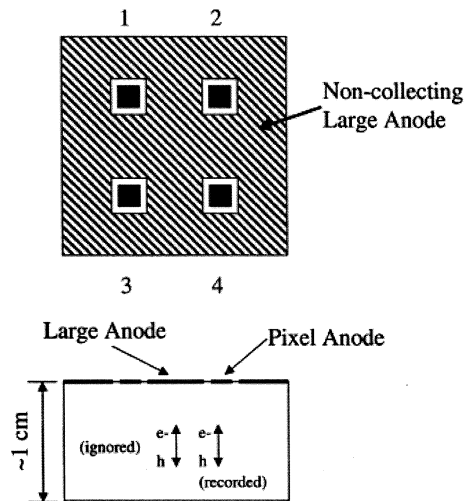
Fig. 1. HgI_2 detector crystal setup (not to scale). Top: top view of anode electrode configuration. Bottom: cross-sectional side view. The cathode and each anode pixel are connected to an Amptek A250 charge sensitive preamplifier. Bias is applied on the cathode and all anodes are grounded. Thus, only events under each pixel are recorded by the anode pixel and events underneath the noncollecting large anode are ignored.

can be obtained by calculating the ratio of the induced charge on each electrode.

In this paper, we present a comparison between 1 cm thick detectors using either planar or pixelated electrodes. Using measured values of mobility and lifetime products for electrons and holes from recently fabricated HgI_2 detectors, we analyzed the theoretical capability of planar and pixelated detectors for gamma-ray spectroscopy using Monte Carlo simulations. The simulated spectra were compared with measured spectra from pixelated HgI_2 detectors.

II. DETECTOR SETUP

Fig. 1 depicts the actual anode pixel configuration used in this work. The four small pixels are surrounded on all sides by a large anode plane. All electrodes are made of palladium. The area of each anode pixel is ~ 1 mm^2 and the total area is approximately 1 cm^2. When the cathode is negatively biased, electrons move toward the anode surface and induce charges on the pixels. The induced signal on the anode is only slightly dependent on the depth of interaction, and is not significantly affected by hole movement. The signal on the planar cathode, on the other hand, is strongly dependent on both hole and electron movement. This effect can be described by the weighting potential for each electrode (Fig. 2).

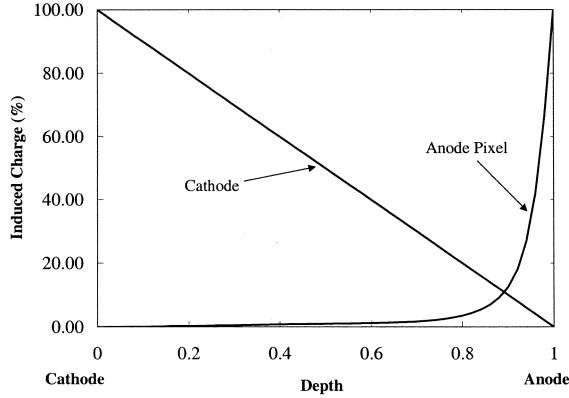0018-9499/03$17.00 © 2003 IEEE

Fig. 2. Weighting potential for a planar cathode and an anode pixel. The cathode has a linear weighting potential and requires the collection of both electrons and holes in order to produce the correct energy spectra. Most of the induced charge for pixelated anodes is produced near the anode. Thus, only electrons need to be collected to produce energy spectra.
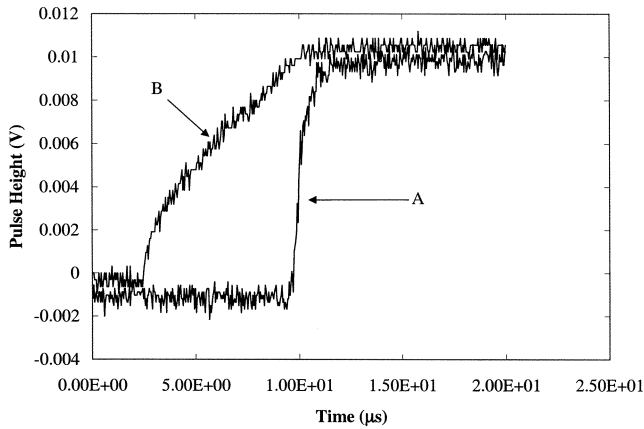

Fig. 3. Pulse waveforms for an event near the cathode. Waveform A is the pixel signal, while waveform B is the cathode signal. Since the electrons can travel the full thickness of the detector the amplitude of the pulse on each electrode is approximately the same. Note that the pixel signal is generated only when the electrons are close to the pixel.

III. ESTIMATION OF MOBILITIES, LIFETIMES, AND DRIFT TIMES OF CHARGE CARRIERS IN MERCURIC IODIDE

The estimation of the electron mobility (μ_e) in HgI$_2$ has been presented previously [6]. The calculation was performed by measuring the electron drift time across the full thickness of a detector. The hole mobility (μ_h) was estimated in a similar manner. An event was chosen such that the interaction took place near the anode pixel surface. Fig. 3 depicts an event near the cathode surface, while Fig. 4 depicts an event near the anode pixel surface. The anode pixel signal has a very sharp slope within one pitch depth of the surface (~ 1 mm). The slower rise of the signal indicates a much lower hole mobility. The signal on the pixel is smaller than the signal generated from electron movement, suggesting either the event was a Compton scatter and/or there was significant hole trapping.

Assuming the holes moved the entire pitch depth, the measured drift time for holes to travel 1 mm was ~ 5 μs. Based upon an electric field of 2500 V/cm, we estimated μ_h to be ~ 8 cm^2/V $-$ s. This value is slightly higher than the generally

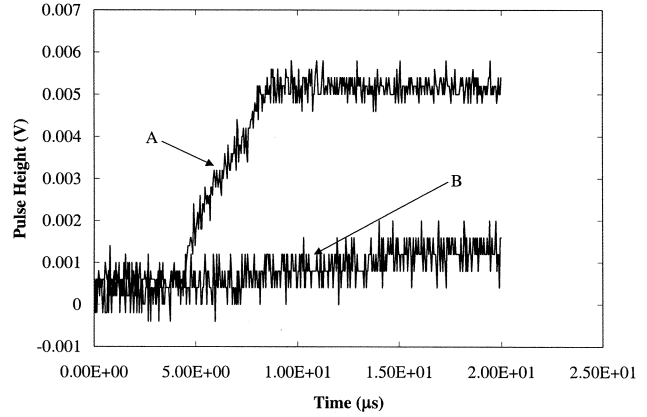accepted value for $\mu_h = 4$ cm^2/V $-$ s for HgI$_2$, and our estimation may have error due to the assumption of a 1 mm pitch depth. This value represents the hole mobility for only one pixel and was not necessarily indicative of the entire crystal. The estimated value $(\mu_h = 8$ cm^2/V$-$s$)$ was incorporated into the simulations for the spectra from planar electrodes presented later in this paper.

The mu-tau product for electrons $(\mu\tau)_e$ was calculated previously [7] using a method first demonstrated on CdZnTe detectors using single polarity charge sensing techniques [8]. While the $(\mu\tau)_e$ varied by approximately one order of magnitude, the pixels with the best resolution generally had the higher $(\mu\tau)_e$. For the purpose of the calculations presented in this paper, we chose a $(\mu\tau)_e = 5 \times 10^{-3}$ cm^2/V.

The mu-tau product for holes was determined by comparing the photopeak from Am-241 60 keV gamma-rays when the detector was irradiated from opposite sides and using a planar cathode (Fig. 5). We started with the general form of the Hecht equation is given by

$$Q = Q_o \left\{ \begin{array}{c} \frac{(\mu\tau)_h E}{D} \left[1 - \exp\left(\frac{-x}{(\mu\tau)_h E} \right) \right] \\ + \frac{(\mu\tau)_e E}{D} \left[1 - \exp\left(\frac{x-D}{(\mu\tau)_e E} \right) \right] \end{array} \right\} \qquad (1)$$

where E is the electric field, x is the interaction distance from the cathode, and D is the detector thickness. For an event near the cathode (i.e., x $\approx$ 0), the Hecht equation reduces to

$$Q_c = Q_o \left\{ \frac{(\mu\tau)_e V}{D^2} \left[1 - \exp\left(\frac{-D^2}{(\mu\tau)_e V} \right) \right] \right\} \qquad (2)$$

where Q_c is the charge (channel number on the ADC) induced on the planar electrode from the cathode irradiation, and V is the bias applied to the detector. A similar result can be obtained for Q_A, the anode irradiation (x $\approx$ D), that only contains the holes term. Taking the ratio of the two equations, we obtain

$$r = \frac{Q_A}{Q_C} = \frac{(\mu\tau)_h \left[1 - \exp\left(\frac{-D^2}{(\mu\tau)_h V} \right) \right]}{(\mu\tau)_e \left[1 - \exp\left(\frac{-D^2}{(\mu\tau)_e V} \right) \right]}. \qquad (3)$$
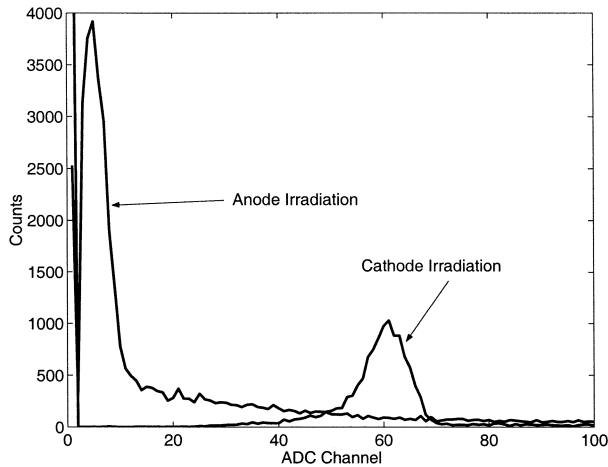
Fig. 5. Am-241 spectra from the cathode signal. The cathode irradiation spectra appeared at a much higher ADC channel since electrons can travel virtually the full thickness of the detector. The peak area for the cathode irradiation was channels 50–70, and 2–10 for the anode irradiation. Note that channel 1 was omitted in the anode irradiation case since it had a large number of counts due to noise.

TABLE I
CALCULATED ELECTRON AND HOLE PARAMETERS FOR MERCURIC IODIDE

μ_e (cm^2/V-s)	τ_e (μs)	μ_h (cm^2/V-s)	τ_h (μs)
67	75	8	3.8

TABLE II
ESTIMATED ELECTRON AND HOLE DRIFT TIMES FOR A 1 CM THICK
MERCURIC IODIDE DETECTOR AT VARIOUS BIASES

Carrier	2.5 kV	5 kV	10 kV
Electrons	5.97 μs	2.99 μs	1.49 μs
Holes	50.0 μs	25.0 μs	12.5 μs

Calculating the peak centroids from first moments of the peak areas, the ratio between the peaks was r ≈ 0.086 for this pixel. Error propagation analysis [9] of this equation revealed an error (σ_r) of about 0.001 or 1%. Solving (3), we obtained a value for $(\mu\tau)_h$ of approximately 3×10^{-5} cm^2/V. The anode irradiation spectrum showed a tailing effect and may have increased the $(\mu\tau)_h$ estimation.

Table I summarizes the results of the estimation of μ_e, μ_h, τ_e, and τ_h for the HgI$_2$ pixelated detectors that we have tested as potential room temperature γ-ray spectrometers. These values were incorporated into the simulations described in the following section. Table II summarizes the calculation of drift times for electrons and holes in HgI$_2$ at three separate biases. From these results, it is clear that it would be advantageous to be able to develop detectors that can generate spectra from only the electron signal as shorter collection times could be used and the significant hole trapping problem can be ignored. Even at 10 kV bias, holes can only effectively travel about 1/3 of the detector thickness.

IV. SIMULATED SPECTRA

Applying the values obtained in the previous section, we simulated spectra that can be obtained from a 1 cm thick HgI$_2$ de-
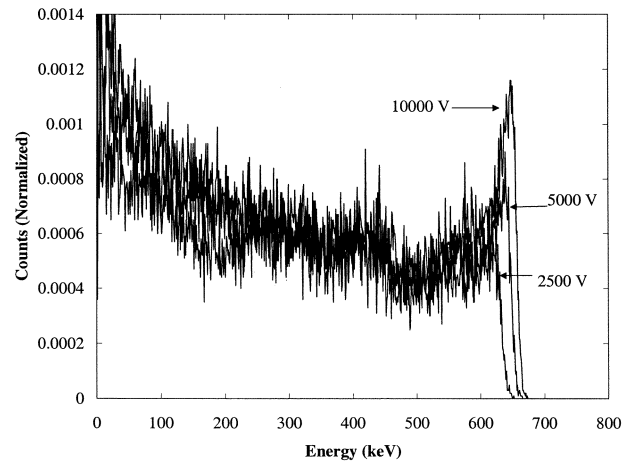

Fig. 6. Simulated Cs-137 spectra from a planar electrode for three biases. Electron and hole movement are both considered.
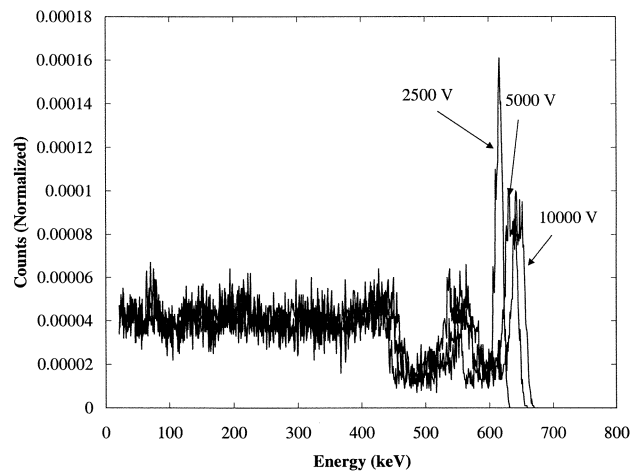

Fig. 7. Simulated Cs-137 spectra from a pixel anode for three biases. The decrease in electron trapping at higher biases causes the pixel weighting potential to be a larger factor in determining the resolution.

tector for both planar and pixelated electrodes. These spectra have assumed that the collection time of the detection system is infinitely long, thus it is an ideal system. Fig. 6 depicts the spectra obtained from a planar electrode with the detector biased at 2.5, 5, and 10 kV using a Cs-137 (662 keV) source. Fig. 7 shows the spectra generated from an anode pixel for the same three biases with the same source while ignoring hole movement within the detector.

From the above figures, the improvement in the planar electrode spectra is clear. As the bias is increased, the amount of holes can travel further before being trapped. This will cause a slightly larger pulse amplitude to be induced on the electrode and shift these events closer to a full 662 keV event. Thus, it is best to use as large an electric field as possible with planar electrodes. The pixelated anode spectra, on the other hand, show a very prominent photopeak event at a relatively low bias. The improvement in the spectra is only marginal at higher biases since electron movement generates all of the induced charge. Electron trapping can compensate for the small amount of depth dependence on the weighting potential. At higher biases, electron
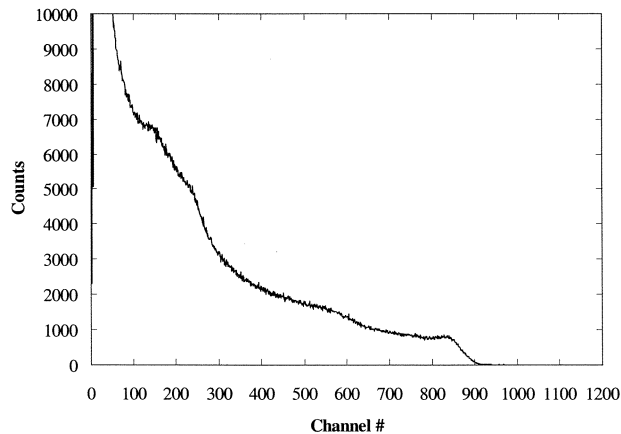
Fig. 8. Cs-137 spectrum collected from the cathode of a 1 cm thick HgI$_2$ detector at a bias of 2500 V. The shaping time used was 16 μs. No peak at 662 keV ($\sim$ channel number 820) was visible.
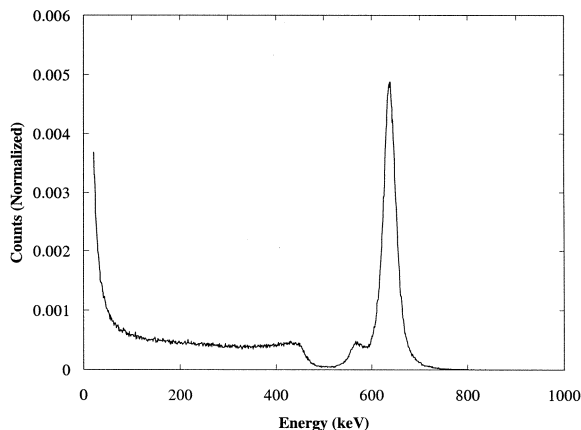

Fig. 10. Simulated Cs-137 spectrum correction for a 1 cm thick HgI$_2$ detector with planar electrodes operating at a bias of 2500 V. By correcting the pulse signal, we can improve the resolution. The resolution here is $\sim$5.3% FWHM. The simulation incorporated a photopeak spread on the same order as the pixels ($\sim$2%).
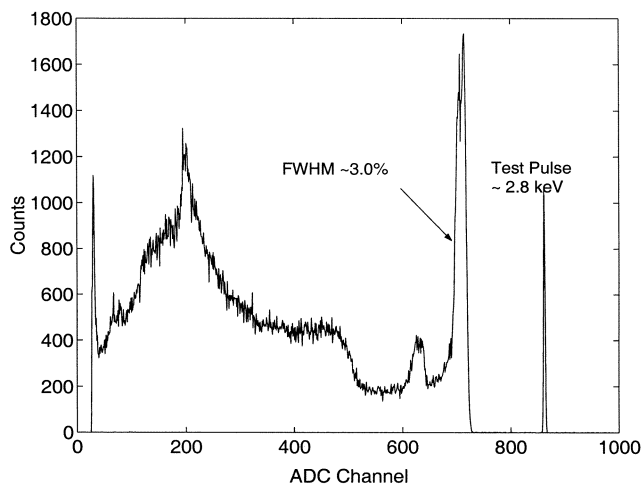

Fig. 9. Cs-137 spectrum obtained from an anode pixel of a 1 cm thick HgI$_2$ detector. The strong photopeak is from electron collection only. Depth correction was not applied. The bias was 2500 V and the shaping time used was 8 μs.

trapping is lower, and the weighting potential becomes a larger factor in determining the resolution. While better hole transportation properties were used in the simulations than generally accepted (slightly higher mobility and lifetime) the simulated spectra from pixels were still better. Thus, using pixelated anodes can allow for the use of lower electric fields without an appreciable loss in resolution or efficiency.

V. GENERATED SPECTRA FROM A CS-137 SOURCE

Using a bias of 2500 V, we tested 1 cm thick HgI$_2$ detectors using pixelated anodes and planar cathodes [10], [11]. These results showed that while a photopeak was not resolvable from the cathode spectra (Fig. 8), the anode pixels were capable of having well resolved photopeaks (Fig. 9).

Despite the lack of a photopeak with the conventional planar electrodes, HgI$_2$ spectra have previously been improved by incorporating pulse compensation techniques [12]. Fig. 10 is a simulated spectrum from a detector using planar electrodes (in

our case, the cathode), assuming the signal can be corrected by knowing the interaction location. The simulation incorporated a photopeak spread on the same order as the anode pixels ($\sim$ 2%). In reality, the leakage current of the large planar electrodes will cause a relatively higher noise, causing the resolution on the planar side to degrade. Even when correcting for the depth of interaction, the resolution will be degraded by the lower signal to noise ratio. For example, at 2500 V applied to a 1 cm thick HgI$_2$ device, events originating near the anode side only induce a charge $\sim$ 1/12 that of an event from near the cathode (this will improve slightly at a higher bias). Thus, the signal to noise is much worse for events near the anode, and the resolution of these events will be poor. The degraded signal from events closer to the anode will contribute to a low- and high-energy tail after applying the correction. Therefore, a detector with conventional electrodes has a tradeoff between energy resolution and detection efficiency since only a fraction of the device can achieve the best resolution.

The spectra of pixelated detectors can also be improved by incorporating the cathode signal with the pixelated anode signal. The cathode signal is highly dependent on the depth of interaction while the anode pixel signal is mainly independent of the depth of interaction. By measuring the cathode to anode signal ratio, we can determine the depth of interaction. The photopeaks from each depth were lined up under the same channel number to correct for the effects of variations in the weighting potential, electron trapping, and potential material nonuniformities that may have affected signal. Fig. 11 depicts the inclusion of depth correction for an anode pixel. The resolution can improve significantly. Of eight pixels tested to date (two 1 cm thick HgI$_2$ detectors), six pixels had a Cs-137 photopeak resolution under 2.0% FHWM, with a best measured resolution of 1.4%. These detectors are able to resolve full photopeak events from nearly the whole thickness of the detector. Two other effects of pixelated anodes can also be seen in Fig. 11. The smaller peak, due to escaped Hg X-rays, was more prominent for pixelated anodes. This is due to the higher probability of the X-rays escaping from the narrow pixel region. Also, the significant number of events that lie between the Compton edge and the photopeak may be
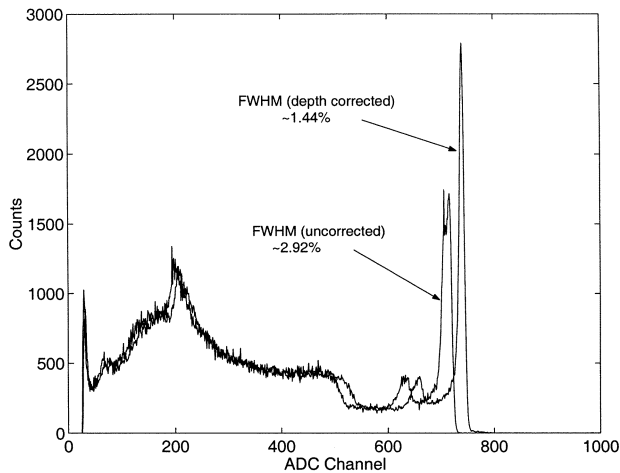
Fig. 11. The inclusion of depth correction by collecting both the anode pixel and planar cathode signals allowed for the correction of weighting potential variations, electron trapping, and material nonuniformity. Here, the 662 keV resolution improved to ~1.4% FWHM.
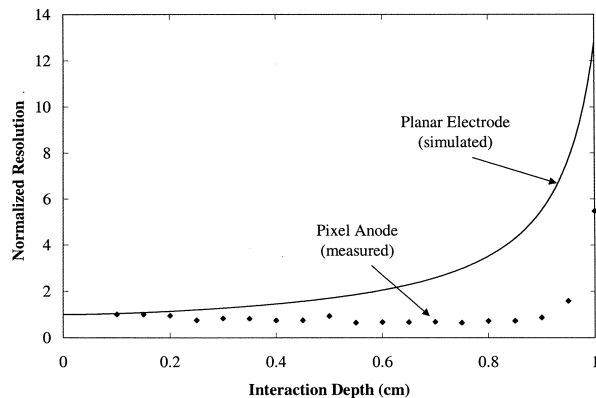

Fig. 12. Resolution as a function of depth for planar and pixelated electrodes, normalized to the resolution for near cathode events.

due to charge sharing. As the electron cloud moves toward the anode, charge diffusion may cause some of the electrons to be collected by the large anode and not be recorded. Photoelectric events which suffered from a significant amount of charge sharing will appear within the region between the Compton edge and the photopeak.

The resolution using pixelated anodes remains relatively constant as a function of depth, whereas the conventional electrode resolution degrades due to the lower signal to noise ratio (Fig. 12). This figure compares resolution results from one of the anode pixels with the best possible resolution from a simulated conventional readout (assuming infinite shaping time to collect induced charge from both hole and electron movement, only single-interaction photopeak events were considered, and assumed a noise the same as that of a pixel anode). The pixelated anode has a resolution that remains relatively constant throughout most of the detector, but the planar electrode signal begins to degrade at approximately 30% of the detector thickness. While these data show the normalized resolution, it should be noted that the actual resolution for pixelated anodes will

be better due to smaller achievable noise. This is due to the smaller capacitance between the electrodes and the sharing of bulk leakage current between the pixels. In reality, Compton scatter events followed by a photoelectric interaction can also contribute to the photopeak. However, these events will further degrade the resolution due to increased errors in determining the depth of interaction for pulse amplitude correction. Inhomogeneities will also contribute more severely to planar electrode spectra that may be overcome by pixelated anodes. The pixelated anodes can compensate for material inhomogeneities that are on the order of 1 mm^2.

VI. CONCLUSION AND FUTURE WORK

Pixelated HgI$_2$ detectors are being tested as potential room temperature γ-ray spectrometers. These thick HgI$_2$ detectors can produce improved spectra than planar electrode HgI$_2$ detectors of similar thickness. Since only electrons need to be collected, pixelated anodes can produce reasonable spectra at a much lower voltage and shorter shaping times than with planar electrodes. Fully pixelated HgI$_2$ detectors can produce full pulse amplitude from a larger fraction of the detector thickness, and thereby maintain the detection efficiency of the detector without sacrificing performance.

While the current results have shown significant improvements in HgI$_2$ detector resolution, we intend to test thick HgI$_2$ devices at higher biases, such as 5 or 10 kV. These future tests should allow for the use of shorter shaping times (2–4 μs) to generate the spectra. The increase in bias will also reduce the amount of electron trapping, and possibly reduce the amount of charge diffusion. Reducing these effects should improve the collection of electrons, and thus the detector performance.

REFERENCES

[1] W. R. Willig, "Mercury iodide as a gamma spectrometer," *Nucl. Instrum. Methods*, vol. 96, pp. 615–616, Nov. 1971.
[2] J. P. Ponpon, "Preliminary results on mercuric iodide nuclear radiation detectors," *Nucl. Instrum. Methods*, vol. 119, July 1974.
[3] H. H. Barrett, "Charge transport in arrays of semiconductor gamma-ray detectors," *Phys. Rev. Lett.*, vol. 75, pp. 156–160, July 1995.
[4] Z. He, W. Li, G. F. Knoll, D. K. Wehe, J. Berry, and C. M. Stahle, "3-D position sensitive CdZnTe gamma-ray spectrometers," *Nucl. Instrum. Methods*, vol. A422, pp. 173–178, Feb. 1999.
[5] Z. He, G. F. Knoll, D. K. Wehe, R. Rojeski, C. H. Mastrangelo, M. Hammig, C. Barrett, and A. Uritani, "1-D position sensitive single carrier semiconductor detectors," *Nucl. Instrum. Methods*, vol. A380, pp. 228–231, Oct. 1996.
[6] Z. He and R. D. Vigil, "Investigation of pixellated HgI$_2$ γ-ray spectrometers," *Nucl. Instrum. Methods*, vol. A492, pp. 387–401, Oct. 2002.
[7] J. E. Baciak, Z. He, and R. P. DeVito, "Electron trapping variations in single-crystal pixelated HgI$_2$ gamma-ray spectrometers," *IEEE Trans. Nucl. Sci.*, vol. 49, pp. 1264–1269, June 2002.
[8] Z. He, G. F. Knoll, and D. K. Wehe, "Direct measurement of $\mu_e \tau_e$ of CdZnTe semiconductors using position sensitive charge sensing detectors," *J. Appl. Phys.*, vol. 84, no. 10, pp. 5566–5569, Nov. 1998.
[9] G. F. Knoll, *Radiation Detection and Measurement*, 3rd ed. New York: Wiley, 1999, pp. 86–92.
[10] J. E. Baciak and Z. He, "Comparison of 5 mm and 10 mm thick HgI$_2$ pixelated γ-ray spectrometers," *Nucl. Instrum. Methods*, vol. 505, pp. 191–194, June 2003.
[11] ——, "Development of a model for gamma-ray spectra generation using pixelated mercuric iodide detectors," in *Proc. SPIE*, vol. 4784, 2002, pp. 119–127.
[12] V. M. Gerrish, D. J. Williams, and A. G. Beyerle, "Pulse filtering for thick mercuric iodide detectors," *IEEE Trans. Nucl. Sci.*, vol. NS-34, pp. 85–90, Feb. 1987.